FTIR Spectroscopic Study of the Adsorption of Hydrogen Cyanide by Metallo-Oxide Pillared Clays

Jim Jamis, Alexander Drljaca, Leone Spiccia, and Thomas D. Smith*

Chemistry Department, Monash University, Clayton, Victoria Australia 3168

Received March 20, 1995. Revised Manuscript Received September 12, 1995[⊗]

The IR spectra due to hydrogen cyanide adsorbed by montmorillonite, montmorillonite pillared by the oxides of aluminum, zirconium, iron, titanium and chromium, montmorillonite pillared by mixed oxides of aluminum/zirconium, chromium/zirconium, iron/zirconium, and chromium/iron/zirconium, acid washed montmorillonite, and acid-washed montmorillonite pillared by oxides of aluminum and zirconium have been recorded at various temperatures of thermal pretreatment of the pillared clays. Similar measurements have been made on hectorite and hectorite pillared by the oxides of aluminum and zirconium. Substantial binding of hydrogen cyanide by Lewis acid sites on the oxide pillars of the clays has been shown to take place after heating the pillared clays to 673 K. The formation of such centres on the oxide pillared montmorillonite falls in the order Al > Ti > Zr ≫ Fe, being undetectable for chromium. The effect of the oxide pillar on the sheet structure of the clay is the production of binding sites on montmorillonite or hectorite similar to those observed in zeolite Y and, additionally, a distinctive site characterized by an IR spectral band in the 2140 cm^{-1} region which is thought to be formed by disruption of the sheet structure with participation of the pillar material. The extent of formation of this site on the sheet structure of montmorillonite increases in the order of the oxides of Al < Fe < Zr < Ti < Cr and again for hectorite its formation is small for pillaring by aluminum oxide and extensive for pillaring by zirconium oxide.

Introduction

Smectite clays have provided the starting material for the creation of microporous molecular sieves by the introduction of cationic hydrolytic polynuclear species into the laminated structure of the clay.[1] When the separation of the layered structure involves polynuclear hydroxy cationic species, introduced by an ion-exchange process onto the negatively charged silicate sheets, subsequent heat treatment of the clay material results in a permanent separation of the sheet structure by metallo-oxide pillars anchored to the silicate sheet by chemical bonding. Such materials have come to be known as pillared inorganic layered compounds (PILC) or cross-linked smectites. Their microporosity arises from the voids between a regular array of metallo-oxidic pillars and metallo-silicate sheets. Early work along with more recent developments in the understanding of pillared clays have been summarized,[1–5] while their roles as catalysts[6] and other uses[7] have been outlined.

Due to the very different chemical composition of the two components of the pillared clays a rational explanation of their chemical behavior is necessarily complex. This is particularly true in considerations of their acidity, which plays an important role in their use as catalysts.[8] Recently, the FTIR spectra due to hydrogen cyanide adsorbed by the protonic forms of zeolites proved useful in identifying the various Brønsted acid sites which engage the hydrogen cyanide by hydrogen bonding resulting in a marked enhancement of the intensity of the IR spectral band due to C≡N stretch (ν_1) along with a shift to higher wavenumber compared with the free gas value.[9] In the gaseous phase, cancellation of large C–H and C≡N bond derivatives in the ν_1 mode of hydrogen cyanide causes this fundamental to be very weak.[10] The increases in IR spectral band intensity, which occur on hydrogen bonding of hydrogen cyanide, have been attributed to dynamic charge transfer and polarization effects accompanying the proton movement in the hydrogen bonded complex.[11] On the other hand, hydrogen bonding of hydrogen cyanide to ammonia results in an increase in the intensity of the ν_1 band with a wavenumber shift to lower values than that of the free gas.[12] This IR spectral shift to lower wavenumbers has been used to discern basic sites responsible for the adsorption of hydrogen cyanide by the heavier alkali metal ion exchanged near-faujasite zeolites.[13]

The present investigation deals with FTIR spectral measurements of hydrogen cyanide adsorbed by pillared clays where both the composition of the metallo-oxide pillar and the sheet structure determine the existence

[⊗] Abstract published in *Advance ACS Abstracts,* October 15, 1995.

(1) Pinnavaia, T. J. *Science* **1983**, *220*, 365.
(2) Rich, C. I. *Clays and Clay Miner.* **1968**, *16*, 30.
(3) Lahav, N.; Shan, U.; Shabtai, J. *Clays Clay Miner.* **1978**, *26*, 107.
(4) Pillared Clays, Burch, R., Ed.; *Catal. Today* **1988**, *2*, 185–367.
(5) Vaughan, D. E. N. *Perspectives on Molecular Sieve Science*; American Chemical Society: Washington, DC , 1988.
(6) Figueras, F. *Catal. Rev. Sci. Eng.* **1988**, *30*, 457.
(7) Mitchell, I. V., Ed. *Pillared Layered Structures*, Elsevier Applied Science: London, 1990.
(8) Bodoardo, S.; Figueras, F.; Garrone, E. *J. Catal.* **1994**, *147*, 223.
(9) Blower, C. J.; Smith, T. D. *J. Chem. Soc., Faraday Trans.* **1994**, *90*, 919.
(10) Marcolcelli, M.; Hopkins, G. A.; Nibler, J. W.; Dyke, T. R. *J. Chem. Phys.* **1985**, *83*, 2129.
(11) Zilles, B. A.; Person, W. B. *J. Chem. Phys.* **1983**, *79*, 65.
(12) Bohn, R. B.; Andrews, L. *J. Phys. Chem.* **1989**, *93*, 3974.
(13) Blower, C. J.; Smith, T. D. *J. Chem. Soc., Faraday Trans.* **1994**, *90*, 931.

0897-4756/95/2807-2078$09.00/0

of hydrogen cyanide receptor sites on the pillar and sheet materials.

Experimental Section

The Clays. Wyoming montmorillonite and hectorite (N.L. Chemicals) were of 200 mesh (<75 μm) particle size fraction. Acid-treated montmorillonite was prepared as described in the literature,[14] starting with sodium-exchanged montmorillonite[15] and sulfuric acid such that the acid concentration during activation was 1.6 mol L^{-1}.

Pillaring Solutions. *Aluminum.* An aqueous solution of sodium hydroxide (AJAX Chemicals, laboratory reagent, 0.2 mol L^{-1}) was added dropwise (0.05 mL s^{-1}) to an aqueous solution of aluminum trichloride (Aldrich, 99%, 0.1 mol L^{-1}) at room temperature (293 K) until an OH/Al ratio of 2.2 was reached. The solution was aged at room temperature for 20 h before use.

Zirconium. An aqueous solution of zirconyl chloride (Aldrich, 98%, 0.1 mol L^{-1}) was aged at 368 K for 8 h before use.

Titanium. Titanium tetrachloride (Aldrich, 99.9%) was added to hydrochloric acid (AJAX Chemicals, analytical reagent, 32%) and diluted by the slow addition of distilled water to reach a titanium concentration of about 0.1 mol L^{-1}. This solution was then aged at room temperature for 3 h before use.

Iron. Crystalline μ_3-oxotriaquohexakis(acetate)triiron(III) chloride was prepared from aqueous solutions containing ferric chloride (AJAX Chemicals, laboratory reagent) and sodium acetate (AJAX Chemicals, laboratory reagent) as described in the literature,[16] and used as an aqueous solution (0.05 mol L^{-1}).

Chromium. (a) An aqueous solution of chromic nitrate (Aldrich, 99%, 0.1 mol L^{-1}) was adjusted to pH 13 by the slow addition of aqueous sodium hydroxide (1.0 mol L^{-1}) with continuous stirring at room temperature which rapidly generates polynuclear anionic Cr(III) species.[17] The solution was then acidified (pH 2.0) by addition of perchloric acid (BDH Chemicals, AR, 70%, 2.0 mol L^{-1}). This procedure converts these anionic species into the corresponding cationic polynuclear species and has previously been used to generate good yields of Cr(III) hydrolytic oligomers.[17] A further solution was prepared after aging of the solution at pH 13 for 5 h with subsequent acidification.

(b) Crystalline μ_3-oxotriaquohexakis(acetate)trichromium-(III) chloride and μ_3-oxotriaquohexakis(formate)trichromium-(III) formate were prepared as described in the literature[16] and used as aqueous solutions (0.05 mol L^{-1}). Pillaring of montmorillonite and hectorite with the chromium(III) formate compound was successful, however, the chromium(III) acetato compound did not exchange into the clays.

(c) The Cr(III) hydrolytic dimer was prepared as described in the literature,[18] and used as an aqueous solution (0.05 mol L^{-1}).

Aluminum/Zirconium. Rezal-67 (Reheis Chemical Co.), an aqueous solution which contains randomly polymerized hydrolytic species of aluminum (2.40 mol L^{-1}) and zirconium (0.355 mol L^{-1}) was used.

Iron/Zirconium. An aqueous solution of sodium hydroxide (1.0 mol L^{-1}) was added dropwise with rapid stirring to an aqueous solution (100 mL) containing ferric nitrate (AJAX Chemicals, laboratory reagent, 0.1 mol L^{-1}) and zirconyl chloride (0.1 mol L^{-1}) until an OH/metal ion ratio of 0.5 was reached. The final solution was aged for 2 h with stirring at 363 K before use.

(14) Mokaya, R.; Jones, W. *J. Chem. Soc., Chem. Commun.* **1994**, 929.
(15) Carr, R. M. *Clays and Clay Miner.* **1985**, *33*, 357.
(16) Earnshaw, A. E.; Figgis, B. N.; Lewis, J. *J. Chem. Soc. A* **1966**, 1656.
(17) Spiccia, L.; Marty, W.; Giovanoli, R. *Inorg. Chem.* **1988**, *27*, 2660.
(18) Merakis, T.; Murphy, A.; Spiccia, L.; Beguin, A.; Marty, W. *Helv. Chim. Acta* **1989**, *72*, 993.

Table 1. Powder XRD Data for the Clays and Pillared Clays[a]

clay material	heat treatment (K) (2 h in air)	basal spacing (d_{001}) (Å)	fwhmh of d_{001} peak (deg)
sodium-mont	R.T.	12.5	0.70
acid treated-mont	R.T.	12.7	0.93
hectorite	R.T.	12.1	2.0
Zr pil-mont	473	16.2	0.92
Al pil-mont	473	17.4	1.1
Ti pil-mont	473	27.8	1.4
Fe pil-mon	473	17.2	1.0
Cr dimer pil-mont	473	13.3	0.75
Cr unaged pil-mont	473	15.2	1.1
Cr aged pil-mont	473	15.6	1.5
Cr formate pil-mont	473	15.0	1.2
Al pil acid-treated-mont	473	15.7	1.6
Zr pil acid-treated-mont	473	17.0	0.86
Al/Zr pil-mont	473	17.7	1.0
Fe/Zr pil-mont	473	19.9	0.65
	773	18.1	0.75
Cr/Zr pil-mont	473	19.4	0.76
	773	18.2	0.80
Cr/Fe/Zr pil-mont	473	19.6	0.80
	773	18.7	0.82
Al pil-hectorite	473	18.3	1.3
Zr pil-hectorite	473	17.3	1.3

[a] Abbreviations: mont ≡ montmorillonite, pil ≡ pillared, fwhmh ≡ full width at half-maximum height of d_{001} basal spacing peak on the 2θ scale.

Chromium/Zirconium. An aqueous solution of sodium hydroxide (1.0 mol L^{-1}) was added dropwise to an aqueous solution (100 mL) containing chromic nitrate (0.1 mol L^{-1}) and zirconyl chloride (0.1 mol L^{-1}) until an OH/metal ion ratio of 1.0 was reached. The final solution was aged for 5 h with stirring at 363 K before use.

Iron/Chromium/Zirconium. An aqueous solution of sodium hydroxide (1.0 mol L^{-1}) was added dropwise to an aqueous solution (100 mL) containing ferric nitrate (0.1 mol L^{-1}), chromic nitrate (0.1 mol L^{-1}) and zirconyl chloride (0.16 mol L^{-1}) until an OH/metal ratio of 2.0 was reached. The final solution was aged for 2 h with stirring at 363 K before use.

The Pillared Clays. Samples (1.0 g) of either sodium montmorillonite or hectorite were dispersed in water (100 mL) and treated with the pillaring solution such that the final metal ion content of the slurry solution was 10 times the cation exchange capacity of the clay. The reaction mixture was stirred for 3 h, and the clay material separated by centrifugation and washed with distilled water until the electrical conductivity of the washings was reduced to less than 5 mS/m.

Powder X-ray Diffraction (XRD) and Surface Area Measurements. Dispersions of the wet clays were spread on glass slides and air dried to form a film which could be heated and kept at the desired temperature (473 or 773 K) for 2 h. The XRD patterns were recorded on a Scintag Pad 5 X-ray diffractometer. The radiation used was a nickel filtered Cu $K\alpha_1$ of wavelength 1.540 59 Å. The instrument was calibrated with a reference silicon powder (National Bureau of Standards). The XRD data were collected on clay samples heated to 473 K. Raising the temperature to 773 K, as shown by selected results in Table 1, caused reductions in the basal spacings.

B.E.T. suface areas of the pillared clays were determined from dinitrogen adsorption isotherms (77 K) using a Carlo-Erba Sorptomatic (Model 1800) apparatus after outgassing (623 K for 16 h) to a residual pressure of 1.0×10^{-4} Torr (1 Torr = 101325/760 Pa).

FTIR Measurements. Infrared spectra were measured using a Perkin-Elmer 1600 spectrometer with 2 cm^{-1} resolution and a 400–4500 cm^{-1} range. Four scans (16 s) of hydrogen cyanide adsorbed by self-supporting wafers of the clays and pillared clays were recorded as described previously.[9] The wafers (15 mg, 15 mm diameter, 0.05 mm thick, compressed by 1500 psi for 15 min and a further 3000 psi for 15

Table 2. B.E.T. Surface Area Measurements for the Pillared Clays

pillared clays	B.E.T. surface areas ($m^2\ g^{-1}$)
Al pil-hectorite	230
Zr pil-hectorite	280
Al pil acid-treated-mont	260
Zr pil acid treated-mont	279
Zr pil-mont	225
Fe pil-mont	280
Al pil-mont	200
Ti pil-mont	320
Cr unaged pil-mont	316
Cr aged pil-mont	347
Al/Zr pil-mont	240
Cr/Zr pil-mont	254
Fe/Zr pil-mont	300
Cr/Fe/Zr pil-mont	260

min) were situated in a cell which allowed control of temperature, gas pressure, and gaseous environment. Deconvolution, derivatization and measurements of area under the curve of the IR spectral bands of interest were carried out using the instrument computer and software. Infrared spectral band areas taken from absorbance measurements (absorbance, which is unitless, multiplied by the wavenumber scale) and normalized to unit mass are expressed as $cm^{-1}\ mg^{-1}$. The preparation and purification of hydrogen cyanide were carried out as described previously.[9] Bearing in mind the highly toxic properties of hydrogen cyanide all operations and final disposal of materials were carried out with due care.

Results

The basal spacings, obtained from the powder XRD data of the clays and pillared clays are shown in Table 1 while measurements of the B.E.T. surface areas of the pillared clays are summarized by Table 2. The FTIR spectra due to hydrogen cyanide adsorbed by wafers of sodium montmorillonite and montmorillonite pillared by various metal oxides (the wafers being initially heated to 473 K before hydrogen cyanide adsorption) were recorded at room temperature over the wavenumber range 2180–2080 cm^{-1} and are shown in Figure 1. In addition, a relatively broad band centered at about 2220 cm^{-1} is observed in the case of the pillared clays. The FTIR spectra due to hydrogen cyanide adsorbed by wafers of acid washed montmorillonite and this form of the clay pillared by oxidic species of aluminum and zirconium are shown in Figure 2, while similar observations made on montmillonite pillared by the mixed oxide combinations aluminum/zirconium, chromium/zirconium, iron/zirconium, and chromium/iron/zirconium are depicted in Figure 3. The FTIR spectral responses of hydrogen cyanide adsorbed by hectorite and hectorite pillared by oxidic species of aluminum or zirconium are shown in Figure 4A.

Increases in the temperature of the initial heat treatment of wafers of the clays and pillared clays leads to decline in the intensity of the IR bands in the 2180–2080 cm^{-1} region but increases in the intensities of the single bands observed in the 2220 cm^{-1} region. These changes in IR spectral intensity of bands due to adsorbed hydrogen cyanide are summarized by Table 3, which deals with the decreasing areas of the bands observed in the 2180–2080 cm^{-1} spectral region, and Table 4, which describes increases in areas which occur for the bands observed in the 2220 cm^{-1} region.

The IR spectral bands due to adsorbed hydrogen cyanide by the pillared clays show changes in shape

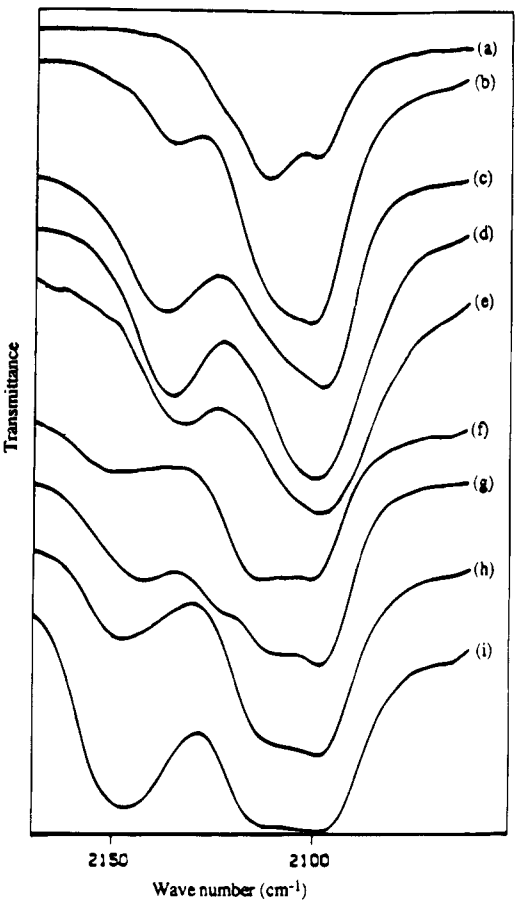

Figure 1. Infrared spectra due to hydrogen cyanide adsorbed by preheated (473 K) wafers of (a) montmorillonite; and montmorillonite pillared by oxides of (b) aluminum; (c) zirconium; (d) titanium; (e) iron (from basic acetate); (f) chromium (dimer hydrolytic form); (g) chromium (basic formate); (h) chromium (unaged); (i) chromium (aged).

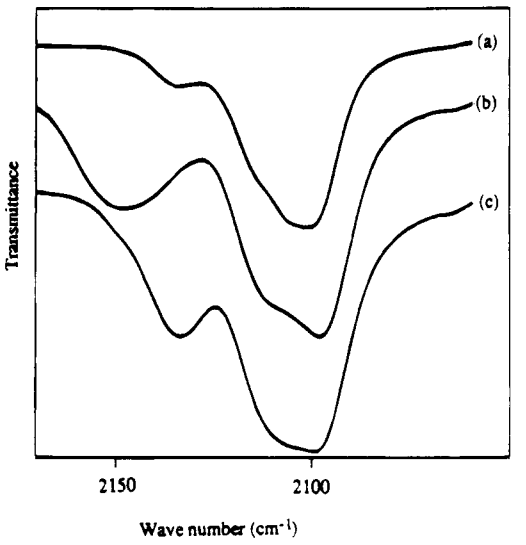

Figure 2. Infrared spectra due to hydrogen cyanide adsorbed by preheated (473 K) wafers of (a) acid-washed montmorillonite; and acid-washed montmorillonite pillared by oxides of (b) aluminum and (c) zirconium.

which are indicative of several spectral components which are easier to observe in the fourth derivative of the spectra. A typical example of such derivatization is depicted by Figure 4B where curvatures are translated into resolved bands.

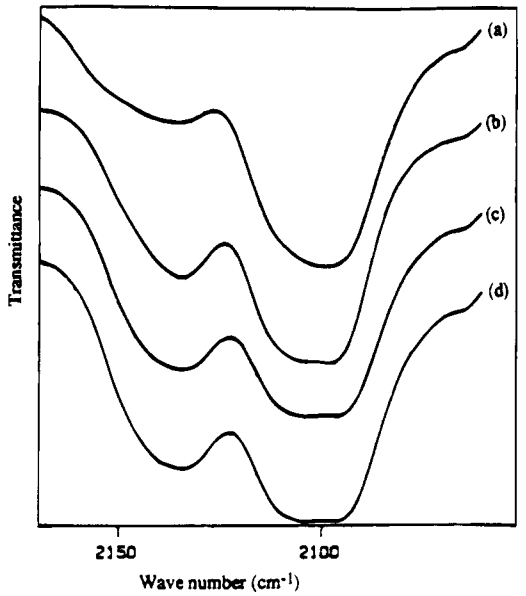

Figure 3. Infrared spectra due to hydrogen cyanide adsorbed by preheated (473 K) wafers of montmorillonite pillared by the mixed oxide combinations (a) aluminum/zirconium; (b) chromium/zirconium; (c) iron/zirconium; (d) iron/chromium/zirconium.

The band positions of the spectral components obtained from derivatization of the IR spectra due to adsorbed hydrogen cyanide on the clays and the various pillared clays are summarized in Table 5. After adsorption of hydrogen cyanide by wafers of the clays and pillared clays, partial removal of the hydrogen cyanide by evacuation leads to a reduction in the intensity of the IR spectral responses in the region 2180–2080 cm^{-1} leading to a simplification of their composite nature. Those components of the IR spectra in this region which survive diminished pressure pumping for 2 min are listed in Table 5. Under the same conditions of diminished pressure desorption of hydrogen cyanide from the pillared clays, very little change in intensity of the band in the 2220 cm^{-1} region occurs.

Losses of hydrogen cyanide from wafers of the clays and pillared clays occur as a result of increasing the temperature of the wafer after exposure to hydrogen cyanide. The results of such thermal desorptions of hydrogen cyanide from wafers initially heated to 473 K are shown in Figure 5 for montmorillonite in the sodium ion and oxidic pillared forms. The wafers were initially heated to 473 K prior to hydrogen cyanide adsorption and then evacuated. Similar results obtained for acid washed and pillared montmorillonite as well as hectorite and pillared hectorite are shown by Figure 6.

Measurements of thermal desorption designed to show the diminished intensity of the bands due to adsorbed hydrogen cyanide on pillared clays in the 2220 cm^{-1} region were made on wafers of the pillared clays initially heated to 673 K. This procedure revealed large peak intensities for this spectral region. The results showed that subsequent heating of the wafers to 573 K was required to remove most of the adsorbed hydrogen cyanide.

To strengthen the view that the IR spectral band in the 2220 cm^{-1} region is due to hydrogen cyanide adsorbed by oxidic material, the IR spectrum due to hydrogen cyanide adsorbed by the protonic form of zeolite Y, steam treated to generate extraframework

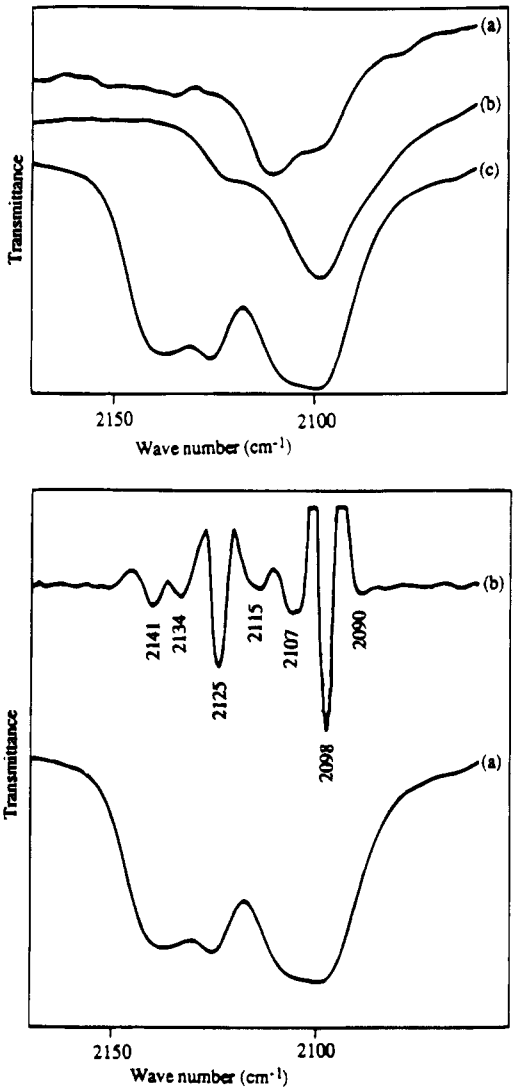

Figure 4. (A, top) Infrared spectra due to hydrogen cyanide adsorbed by preheated (473 K) wafers of (a) hectorite and hectorite pillared by the oxides of (b) aluminum and (c) zirconium. (B, bottom) Infrared spectra due to hydrogen cyanide adsorbed by a preheated (473 K) wafer of (a) hectorite pillared by zirconium oxide; (b) fourth derivative of spectrum (a).

alumina,[9] was recorded and compared with the IR spectrum due to hydrogen cyanide adsorbed by heat treated alumina. The results, obtained after removing the less tenaciously held hydrogen cyanide by partial evacuation, are illustrated by Figure 7 and show the presence of the IR spectral band in the 2220 cm^{-1} region for both adsorbents.

Discussion

An increased separation of silicate layers of the smectite clays is achieved as a result of an ion-exchange process involving their heterogeneous cation sites[19,20] and polynuclear hydrolytic species of the multivalent cations. Studies of the hydrolysis of cations of aluminum,[21] zirconium,[22,23] titanium,[24] and chromium[17] have

(19) Stul, M. S.; Mortier, W. J. *Clays Clay Minerals* **1974**, *22*, 391.
(20) Peigneur, P.; Maes, A.; Creners, A. *Clays Clay Minerals* **1975**, *23*, 71.
(21) Akitt, J. W.; Elders, J. M. *J. Chem. Soc., Dalton Trans.* **1988**, 1347.
(22) Lister, B. A. J.; McDonald, L. A. *J. Chem. Soc.* **1952**, 4315.

Table 3. Decreasing Total Areas of the IR Spectral Bands in the Region 2180–2080 cm^{-1} Due to Hydrogen Cyanide Adsorbed by Wafers of the Clays and Pillared Clays Preheated to Various Temperatures

	hydrogen cyanide peak areas (cm^{-1} mg^{-1}) at different temp			
clays and pillared clays	473 K	533 K	603 K	673 K
hectorite	0.29	0.24	0.22	0.21
Al pil-hectorite	0.74	0.58	0.48	0.28
Zr pil-hectorite	1.81	1.73	1.12	1.04
acid-treated-mont	0.39	0.32	0.29	0.24
Al pil acid-treated-mont	0.79	0.70	0.61	0.45
Zr pil acid-treated-mont	1.07	0.91	0.61	0.47
sodium-mont	0.33	0.28	0.25	0.23
Zr pil-mont	0.82	0.67	0.57	0.43
Fe pil-mont	1.01	0.86	0.75	0.64
Al pil-mont	1.06	0.93	0.80	0.65
Ti pil-mont	1.08	1.00	0.89	0.80
Cr-aged pil-mont	1.21	1.06	0.92	0.80
Al/Zr pil-mont	1.20	1.14	0.92	0.71
Cr/Zr pil-mont	1.30	1.23	1.18	1.06
Cr/Fe/Zr pil-mont	1.49	1.24	1.05	0.71
Fe/Zr pil-mont	1.60	1.56	1.53	1.46

Table 4. Increasing Peak Areas of the IR Spectral Band in the Region 2220 cm^{-1} Due to Hydrogen Cyanide Adsorbed by Wafers of the Pillared Clays Preheated to Various Temperatures

		hydrogen cyanide peak areas (cm^{-1} mg^{-1}) at different temp			
pillared clays	wavenumber (cm^{-1})	473 K	533 K	603 K	673 K
Al pil-hectorite	2217	0.29	0.40	0.51	0.79
Zr pil-hectorite	2220	0.08	0.26	0.49	0.56
Al pil acid-treated-mont	2220	0.03	0.09	0.22	0.31
Zr pil acid-treated-mont	2219	0.03	0.22	0.25	0.35
Zr pil-mont	2220	0.03	0.11	0.22	0.23
Fe pil-mont	2220	0.07	0.03	0.08	0.09
Al pil-mont	2218	0.09	0.16	0.51	0.67
Ti pil-mont	2216	0.17	0.17	0.18	0.29
Al/Zr pil-mont	2217	0.16	0.33	0.60	0.72
Cr/Zr pil-mont	2219	0.14	0.20	0.37	0.58
Cr/Fe/Zrpil-mont	2220		0.02	0.07	0.12
Fe/Zr pil-mont	2220	0.02	0.07	0.17	0.22

shown the existence of a distribution of hydrolytic species. Where evidence has been presented for the existence of clearly defined hydrolytic products such as $[AlO_4Al_{12}(OH)_{24}(OH_2)_{12}]^{7+}$,[25-27] $[Zr_4(OH)_8(OH_2)_{16}]^{8+}$,[28,29] or more recently $[Zr_{18}O_4(OH)_{36}(OH_2)_{16}]^{28+}$,[30] $[(TiO)_8(OH)_{12}]^{4+}$,[24] $[(H_2O)_4Cr(\mu\text{-}OH)_2Cr(OH_2)_4]^{4+}$,[18,31] and $[Cr_3(\mu\text{-}OH)_4(OH_2)_9]^{5+}$,[17,31] these species have been thought to play an important role in the exchange process. Subsequent heat treatment results in dehydration of the metal hydroxide pillars which hold the clay layers in place to form slitlike micropores whose pore volume depends on the space between the pillars and their height. Additionally, there is a reduction in the charge of the pillar material with a compensatory transfer of protons to the clay sheets. In the case of the pillaring of beidellite and fluorohectorite, the pillars are fastened to the tetrahedral components of the clay sheet by covalent bonds.[32,33] Linking of alumina and zirconia in pillared montmorillonite has been concluded to involve the aluminum and magnesium atoms in the octahedral components of montmorillonite layer after calcination at high temperatures,[34] and heat treatment at lower temperatures may result in a less defined linkage of pillar to the clay layer.[35] In the case of clearly defined Cr(III) oligomers (dimer–hexamer) evidence for the covalent attachment of the polyoxocation to the clay layers has also been observed.[31] The calcined materials, though poorly crystalline,[33] may be considered to be a two-dimensional zeolite.[32] The salient features in terms of basal spacings, cation-exchange capacity, surface areas and conditions of syntheses of the pillared clays which are of interest here have been described in the literature for montmorillonite pillared by aluminum oxide,[36-38] zirconium oxide,[39,40] titanium oxide,[41] iron oxide,[42,43] chromium oxide,[15,44,45] iron/aluminum mixed oxide,[46] and saponite pillared by aluminum oxide.[47] In considerations of the acidic properties of pillared clays the important contribution of the pillars to Lewis acidity has been recognized.[48] A thorough water washing of the pillared clays prior to calcination is an essential prerequisite to obtaining materials characterized by well-defined powder XRD bands whose sharpness is specified here by small values of the full width at half maximum height in units of 2θ (Table 1). The basal spacings data obtained in this work (Table 1) is in good agreement with literature data. The B.E.T. surface area measurements on the metal oxide pillared clays (Table 2) are comparable to those reported in the literature for some of these materials.

The overall IR spectral features of hydrogen cyanide adsorbed by the pillared clays initially heated to 473 K are two bands in the 2180–2080 cm^{-1} region and a much smaller band at about 2220 cm^{-1}. Within the region 2180–2080 cm^{-1}, a band occurs over the range 2150–2134 cm^{-1} while the broad band in the 2125–2080 cm^{-1} region is a combination of three component bands centered at 2114, 2108, and 2099 cm^{-1}. The band

(23) Johson, J. S.; Kraus, K. A. *J. Am. Chem. Soc.* **1956**, *78*, 3937.
(24) Einaga, H. *J. Chem. Soc., Dalton Trans.* **1979**, 1917.
(25) Johannson, G. *Acta Chem. Scand.* **1952**, *6*, 910.
(26) Rausch, W.; Bale, W. D. *J. Chem. Phys.* **1964**, *40*, 3891.
(27) Bottero, J. Y.; Axelos, M.; Tchoubar, D.; Cases, J. M.; Fripiat, J. J.; Fiessinger, F. *J. Colloid. Interface Sc.* **1987**, *117*, 47.
(28) Clearfield, A.; Vaughan, P. A. *Acta Crystallogr.* **1956**, *9*, 555.
(29) Muha, G. N.; Vaughan, P. A. *J. Chem. Phys.* **1960**, *33*, 194.
(30) Squattrito, P. J.; Rudolf, P. R.; Clearfield, A. *Inorg. Chem.* **1987**, *26*, 4240.
(31) Drljaca, A.; Anderson, J. R.; Spiccia, L.; Turney, T. W. *Inorg. Chem.* **1992**, *31*, 4894.
(32) Plee, D.; Borg, F.; Gatineau, L.; Fripiat, J. J. *J. Am. Chem. Soc.* **1985**, *107*, 2362.
(33) Fripiat, J. J. *Catal. Today* **1988**, 291.
(34) Tennakoon, D. T. B.; Jones, W.; Thomas, J. M. *J. Chem. Soc., Faraday Trans. I* **1986**, *82*, 3081.
(35) Pinnavaia, T. J.; Sandan, S. D.; Tzou, M.-S.; Johnson, I. D.; Lipsicus, N. *J. Am. Chem. Soc.* **1985**, *107*, 7222.
(36) Lahav, N.; Shani, U.; Shabtai, J. *Clays and Clay Miner.* **1978**, *26*, 107.
(37) Pinnavaia, T. J.; Tzou, M.-S.; Landau, S. D.; Raythatha, R. H. *J. Mol. Catal.* **1984**, *27*, 195.
(38) Stacey, M. H. *Catal. Today* **1988**, *2*, 621.
(39) Yamanaka, S.; Brindley, G. W. *Clays Clay Miner.* **1979**, *27*, 199.
(40) Burch, R.; Warburton, C. I. *J. Catal.* **1986**, *97*, 503.
(41) Sterte, J. *Clays Clay Miner.* **1986**, *34*, 658.
(42) Doff, D. H.; Gangas, N. H. J.; Allan, J. E. N.; Coey, J. M. D. *Clay Miner.* **1988**, *23*, 367.
(43) Yamanaka, S.; Doi, T.; Sako, S. Hattori, M. *Mater. Res. Bull.* **1984**, *19*, 161.
(44) Pinnavaia, T. J.; Tzou, M.-S.; Landau, S. D. *J. Am. Chem. Soc.* **1985**, *107*, 4783.
(45) Volzone, C.; Cesio, A. M.; Torres Sanchez, R. M.; Pereira, E. *Clays Clay Miner.* **1993**, *41*, 702.
(46) Znao, D.; Wang, G.; Yang, Y.; Guo, X.; Wang, Q.; Ren, J. *Clays Clay Miner.* **1993**, *41*, 317.
(47) Schooheydt, R. A.; van den Eynde, J.; Tabbax, H.; Leeman, H.; Stuyckens, M.; Lenotte, I.; Stone, W. E. E. *Clays Clay Miner.* **1993**, *41*, 598.
(48) Ming-Yuan, H.; Zhonghui, L.; Enze, M. *Catal. Today* **1988**, *2*, 321.

Table 5. Wavenumbers of the Spectral Components of the IR Spectral Bands in the Region 2080–2180 cm^{-1}

clay material	constituent peaks (cm^{-1})						constituent peaks (cm^{-1}) after pumping			
sodium-mont	2098		2108	2111	2123			2108	2124	
Zr pil-mont	2099	2104	2108	2114	2134	2146		2106	2134	2146
Al pil-mont	2099	2106		2114		2140	2104			
Ti pil-mont	2099	2106	2108	2115	2134		2101		2134	
Fe pil-mont	2099	2105		2110	2131		2101		2130	
Cr dimer pil-mont	2098	2106		2114		2150		2111		2150
Cr formate pil-mont	2098	2106		2112		2140		2108		2140
Cr unaged pil-mont	2098	2104	2108	2114		2148		2108		2148
Cr aged pil-mont	2099	2106		2115		2147		2107		2148
acid treated-mont	2098		2107	2115	2136			2109	2136	
Al pil acid-treated-mont	2098		2108	2114		2149		2107		
Zr pil acid-treated-mont	2098		2108	2114	2132			2106		
Al/Zr pil-mont	2099	2104	2108	2114	2136	2152	2103	2108	2136	2152
Cr/Zr pil mont	2099	2104		2114	2135	2152	2104		2135	
Fe/Zr pil-mont	2099	2104	2108	2114	2132		2104		2132	
Cr/Fe/Zr pil-mont	2099		2106	2114	2133		2102			
hectorite	2098	2104	2108	2114			2104	2114		
Al pil-hectorite	2098	2104			2122		2102		2123	
Zr pil-hectorite	2098		2107	2114	2125	2137		2107	2125	2137

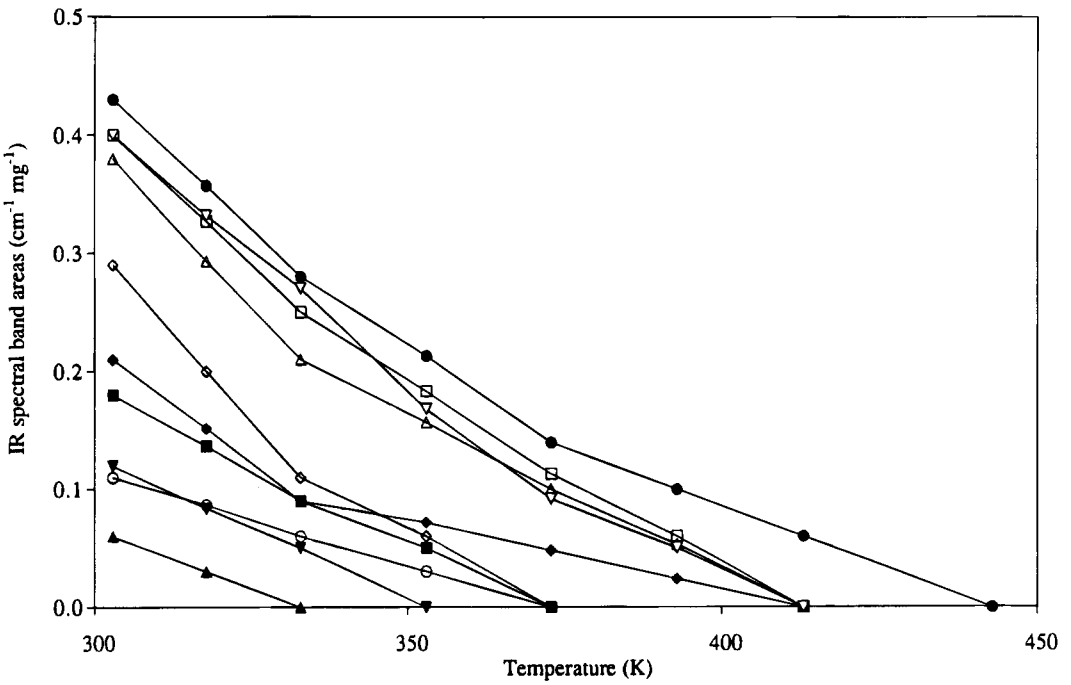

Figure 5. Decreasing areas of the infrared spectral peaks in the 2180–2080 cm^{-1} region, which survive diminished pressure pumping, due to hydrogen cyanide adsorbed by preheated (473 K) wafers of (a) montmorillonite (▲), and montmorillonite pillared by the oxides of (b) zirconium (○) (c) aluminum (■) (d) aluminum/zirconium (◇), (e) chromium/zirconium (△), (f) iron/chromium/zirconium (□), (g) iron/zirconium (●), (h) titanium (▼), (i) iron (acetate) (♦), (j) chromium (aged) (▽).

at 2108 cm^{-1} is often accompanied by a band at 2104 cm^{-1}.

The band centered close to 2220 cm^{-1} grows in intensity with increasing temperature of thermal treatment of the pillared clay prior to hydrogen cyanide adsorption (Table 4). This mode is absent for sodium montmorillonite and chromium oxide pillared montmorillonite. Its intensity is little affected by evacuation and requires a relatively high temperature to reduce its intensity. These distinctive properties of wavenumber and tenacious binding of hydrogen cyanide are attributable to the existence of Lewis acid centers on the oxidic pillar materials which form chemical coordinate bonds to the nitrogen atoms of the hydrogen cyanide resulting in wavenumber shifts due to its ν_1 vibration from the free gas value. These sites are formed in significant amounts at 673 K which may be compared with the binding of hydrogen cyanide by steamed alumina and the extraframework material formed in steamed Y zeolite.[9] For pillared montmorillonite the extent of formation of such centers falls in the order of Al > Ti > Zr ≫ Fe being undetectable for pillaring by chromium oxide. However, the formation of Lewis acid sites on the oxidic pillar is more than halved for alumina but somewhat increased for zirconium oxide pillars when using acid washed montmorillonite. Again, the oxidic pillar material containing aluminum or zirconium develops more Lewis acidity over the whole temperature range when distributed between the clay sheets of hectorite compared with montmorillonite. An enhancement in the formation of Lewis acid sites is attributable to the presence of zirconium oxide in the mixed aluminum/zirconium oxide pillar material. This improvement in Lewis site formation is also observed when a mixed chromium/zirconium oxide pillar is used rather than a zirconium oxide pillar. However, the introduction of iron oxide in the zirconium/chromium/iron oxide pillar combination causes a sig-

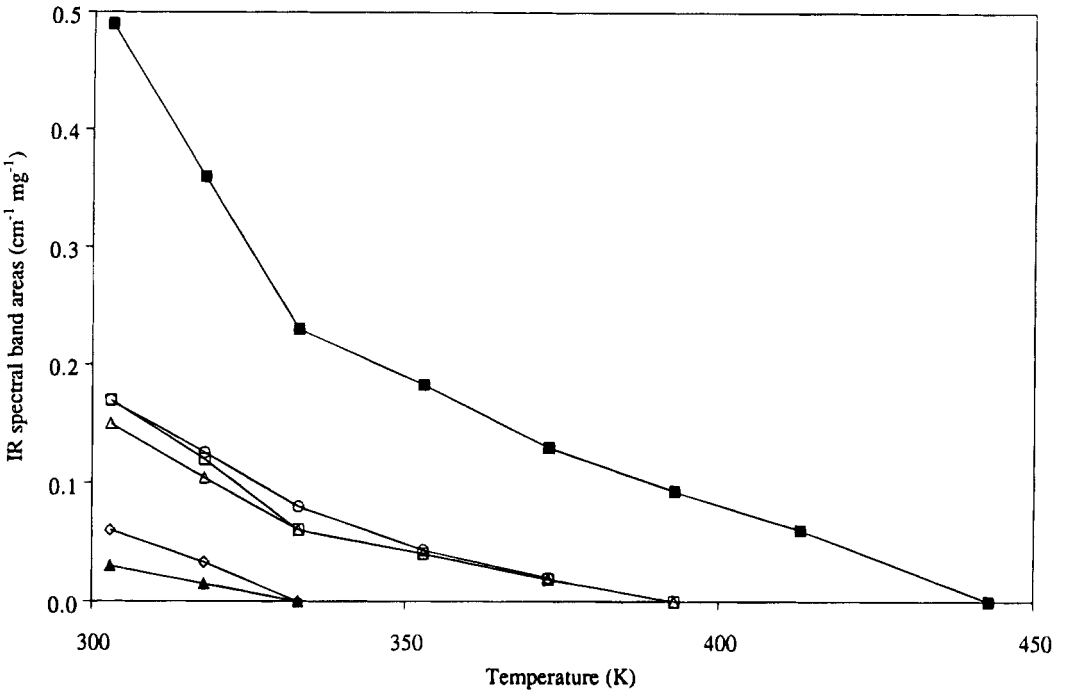

Figure 6. Decreasing areas of the infrared spectral peaks in the 2180–2080 cm^{-1} region, which survive diminished pressure pumping, due to hydrogen cyanide adsorbed by preheated (473 K) wafers of (a) hectorite (▲), hectorite pillared by the oxides of (b) aluminum (○), (c) zirconium (■), (d) acid-washed montmorillonite (◇), and acid-washed montmorillonite pillared by the oxides of (e) aluminum (△), (f) zirconium (□).

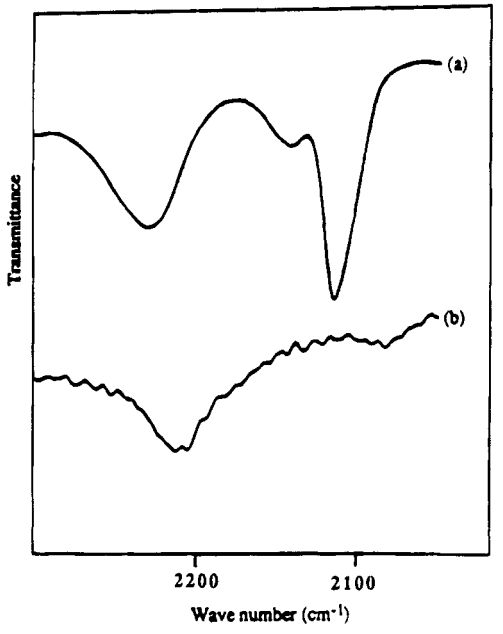

Figure 7. Infrared spectra due to hydrogen cyanide adsorbed by preheated (673 K) wafers of (a) steam treated (873 K) zeolite Y (b) preheated (673 K) chromatographic grade neutral alumina. Both spectra were recorded after partial removal of hydrogen cyanide by pressure desorption for 2 min at 0.001 Torr.

nificant reduction in Lewis site formation, which may arise from structural defects in the oxide structure.

In the case of the adsorption of hydrogen cyanide by zeolites, the appearance of the IR bands due to adsorbed hydrogen cyanide is accompanied by the progressive disappearance or shift of bands in the hydroxyl region. Similarly, for the pillared clays their bands in the hydroxyl region are affected by the presence of hydrogen cyanide. The reduction of the intensity of bands in the 2180–2080 cm^{-1} region (due to adsorbed hydrogen cyanide, after short periods of evacuation) and the relatively low temperatures of thermal desorption (to remove the remaining hydrogen cyanide) along with the wavenumbers of the IR bands indicate binding of hydrogen cyanide by Brønsted acid sites. Thermal desorption, which removes the tightly bound hydrogen cyanide represented by bands in the 2108 and 2140 cm^{-1} regions, distinguishes the strength of binding of hydrogen cyanide as indicated by Figures 5 and 6. The steeper parts of the thermal desorption curves involve mostly reductions in the intensity of IR bands in the 2108 cm^{-1} region while the less steep portion of the curves results from loss in intensity of the IR bands in the 2140 cm^{-1} region which represents the tightly bound hydrogen cyanide. The bonding of hydrogen cyanide by the Brønsted acidity of the pillared clays may be divided into weak (2098, 2114 cm^{-1}), intermediate (2108 cm^{-1}), and strong (2140 cm^{-1}). The weak and intermediate strength of binding of hydrogen cyanide by the pillared clays resembles those observed in the zeolites, particularly the near-faujasite zeolites. However, these sites are present to a limited extent on the parent clays. Acid treatment of montmorillonite enhances their presence and, very importantly, generates a new site to a small extent represented by the band at 2136 cm^{-1} as a result of some breakdown of the clay sheet structure. In terms of active sites for the adsorption of hydrogen cyanide what pillaring achieves is the distinctive formation of a strong binding site (2140 cm^{-1}) which gives the distribution of acid sites a distinctive character. As indicated by Table 3, this achievement is greatly influenced by the nature of the metal oxide involved in the pillaring process and illustrated in Figure 1. The results shown in Figures 5 and 6 focus largely on the influence of the pillaring material on the increased binding of hydrogen cyanide by the stronger receptor

sites (2108, 2140 cm^{-1}). For the chromium oxide pillared materials, the intensity of the band at 2148 cm^{-1} is strongly influenced by the hydrolytic processing conditions used to prepare the pillaring material. Figure 1 shows that the band increases in the order chromium dimer, chromium unaged polymer, and chromium-aged polymer with chromium hydroxyformate resulting in a shift of the band to lower wavenumbers. In the case of uptake of hydrogen cyanide by mixed oxide pillared forms of montmorillonite the wavenumber and intensity of this peak is determined largely by the zirconium oxide content of the pillar material. X-ray crystallographic evidence has been presented for the formation of a $Zr_6Cr_4O_8(OH)_8$ unit in zirconium/chromium basic sulfates.[49]

The adsorption of hydrogen cyanide by the clay sheet surface arises from its hydrogen bonding by the Brønsted acid sites on the clay sheet. This results in an increase in the intensity of the ν_1 band and a shift to higher wavenumbers. The narrow spectral band widths enables the detection of various kinds of Brønsted acid sites. Similarly coordinate bonding of hydrogen cyanide by Lewis acid centres on the oxidic pillar material is marked by a distinctive, relatively broader spectral band at much higher wavenumbers compared with the free gas value.

While most of the spectral bands due to adsorbed hydrogen cyanide on the clay sheet are similar to those encountered in studies of hydrogen cyanide adsorbed on zeolites,[9] in the case of montmorillonite two distinctive bands in the 2080–2180 cm^{-1} region (due to tenaciously held hydrogen cyanide) mark the formation of two new Brønsted acid sites on the pillared clays which are not present on the unpillared material. Their occurrence is such that all the pillared montmorillonites have one or other of such new sites while some (for example, zirconium oxide pillared montmorillonite) have both. One of these bands which occurs at about 2134 cm^{-1} is also generated by acid treatment of montmorillonite and marks the extra Brønsted acidity which enhances the hydrocarbon activity of this material and indicates that the pillaring process is equivalent to acid washing though it is more successful in the generation of this site.

It is proposed that the IR spectral band in the 2140 cm^{-1} region which arises from the hydrogen bonding of hydrogen cyanide by a new Brønsted site and whose intensity may be taken as a guide to the characteristics of the pillaring process on the sheet structure of the clay, is due to a disruptive short-order structural change in the silicate sheet of the clay which serves as a receptor site for the hydrogen cyanide and increases in amount in the order of pillaring by the oxides of Al < Fe < Zr < Ti < Cr. The shift of this IR spectral band to higher wavenumbers in the case of the pillaring by chromium oxide suggests that the pillar material is part of the receptor site. While pillaring of montmorillonite by aluminum oxide has a minimal influence on its sheet structure as shown by Figure 1, the marked increase in the intensity of the IR band at 2148 cm^{-1} indicates that acid washing of the montmorillonite results in the sheet structure becoming more susceptible to modification by the pillar material which itself, as shown by Table 3, is modified so as to develop a reduced level of Lewis acidity at higher temperatures. That this site essentially belongs to the sheet structure of montmorillonite is further demonstrated by its absence in the pillaring of hectorite. The effect of the sheet structure of hectorite, the trioctahedral analogue of montmorillonite with principally octahedral substitutions of Li^+ for Mg^{2+} ions, as indicated by Table 3, is to encourage the formation of Lewis acid sites at the higher temperatures of thermal treatment. The effect of the oxide pillar on the sheet is minimal for aluminum oxide giving an IR spectral band of modest intensity at 2111 cm^{-1} while for zirconium oxide, IR bands of much greater intensity are observed at 2125 and 2137 cm^{-1} with the latter band being resolved into bands at 2141 and 2134 cm^{-1}. These observations once more point to structural change in the silicate sheets with the production of a distinctive receptor site for hydrogen cyanide which involves the pillar component and disrupted silicate sheet material.

Acknowledgment. This work was supported by the Australian Research Council. A.D. acknowledges financial support in the form of an Australian Postgraduate Research Award.

CM950128T

(49) Gatehouse, B. M.; Platts, S. N. *Aust. J. Chem.* **1993**, *46*, 1.